Mech. Sci., 3, 85–93, 2012
www.mech-sci.net/3/85/2012/
doi:10.5194/ms-3-85-2012

Mechanical Sciences
Open Access

A statically balanced and bi-stable compliant end effector combined with a laparoscopic 2DoF robotic arm

J. Lassooij[1], N. Tolou[1], G. Tortora[2], S. Caccavaro[2], A. Menciassi[2], and J. L. Herder[1]

[1]Delft University of Technology, Faculty of Mechanical, Maritime and Materials Engineering, Department of Biomechanical Engineering, Mekelweg 2, 2628 CD Delft, The Netherlands
[2]The BioRobotics Institute, Scuola Superiore Sant'Anna, Piazza Martiri della Libertà 33, 56127 Pisa, Italy

Correspondence to: N. Tolou (n.tolou@tudelft.nl)

Received: 31 March 2011 – Revised: 22 August 2011 – Accepted: 22 October 2011 – Published: 5 December 2012

Abstract. This article presents the design of a newly developed 2DoF robotic arm with a novel statically balanced and bi-stable compliant grasper as the end effector for laparoscopic surgery application. The arm is based on internal motors actuating 2 rotational DoFs: pitch and roll. The positive stiffness of the monolithic grasper has been compensated using pre-curved straight guided beams that are preloaded collinear with the direction of actuation of the grasper. The result is a fully compliant statically balanced laparoscopic grasper. The grasper has been successfully adapted to a robotic arm. The maximum force and stiffness compensations were measured to be 94 % and 97 % (i.e. near zero stiffness) respectively. Furthermore, the feasibility of adjusting for bi-stable behavior has been shown. This research can be a preliminary step towards the design of a statically balanced fully compliant robotic arm for laparoscopic surgery and similar areas.

1 Introduction

In recent years, surgical technologies have been advancing with many devices proposed to reduce the invasiveness of surgery (Breedveld, 1999). The main benefit of minimally invasive surgery (MIS) derives from the small incisions needed to perform complex procedures, thus reducing patient trauma and leading to shortened recovery times and improved cosmetics compared to open procedures (Forgione, 2009). Conventional MIS is performed by means of long slender instruments. Nowadays, laparoscopy represents the standard technique in surgery, but it requires high skills for two main reasons: (1) lost hand-eye-coordination and reduced freedom of movement, and (2) missing direct manual contact to the operation area. Therefore, many sophisticated procedures still cannot be performed minimally invasively. Robotic surgery and compliant mechanisms (CM) play important roles in overcoming the drawbacks of conventional MIS. In current robotic platforms the tools, are not manipulated directly by the surgeon anymore, but are held by specialized robot arms and remotely commanded by the surgeon who comfortably sits at an input console, such as in the Intuitive Surgical's da Vinci system (Alterovitz, 2009) and in the RAVEN robotic platform for telesurgery (Lum et al., 2009). An alternative approach is to introduce small robots with embedded actuators inside the body, as demonstrated by several researchers (Rentschler et al., 2006; Hu et al., 2009; Fowler et al., 2010; Lehman et al., 2008; Oleynikov et al., 2005).

Compliant mechanisms can help in overcoming the second drawback, i.e. missing direct manual contact to the operation area. Because the surgeon has to use long slender instruments instead of manually feeling the tissue, the sense of force feedback is lost. This is mainly due to the large amount of friction in laparoscopic graspers, and is the main reason of increased errors made by surgeons (Joice, 1998). Compliant mechanisms do not use rigid body joints to gain part or all of their motion. Instead, they use the relative flexibility of their members (Howell, 2001). Therefore, these mechanisms offer several advantages, including single-piece production, absence of Coulomb friction, no need for lubrication, and compactness, compared to conventional rigid body mechanisms. However, the energy storage in the compliant mechanism can be a big drawback, because the input-output relationship is affected; part of the input energy is not transferred

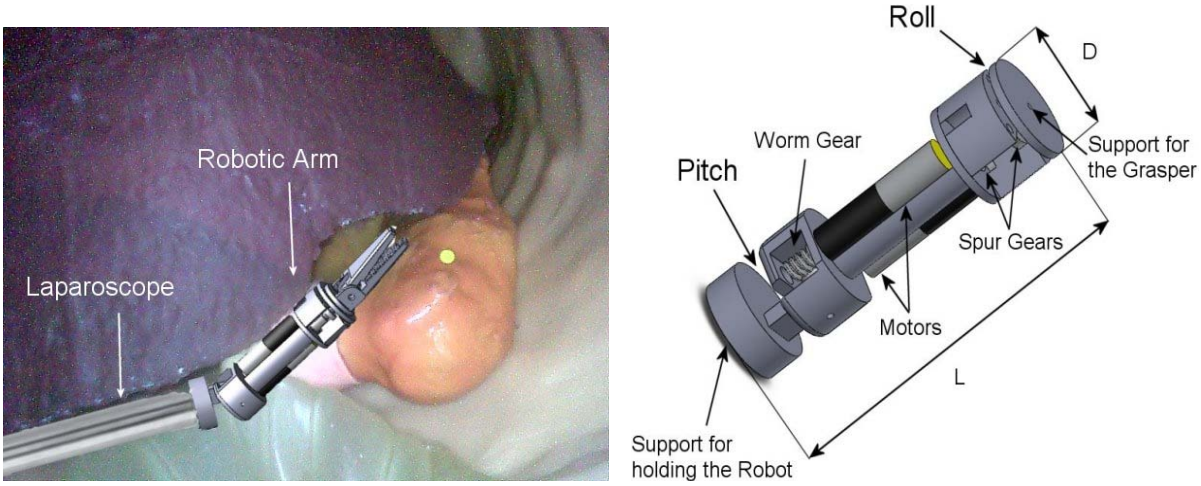

Figure 1. **(a)** View of the robot in a possible working scenario in a phantom with silicone organs (provided by EndoCAS Center, Pisa, Italy); the grasper will be substituted by the compliant grasper of Fig. 2; **(b)** 3-D sketch of the robot.

to the output, but used for the deformation of the compliant segments of the mechanism (Tolou et al., 2010a). Especially in the laparoscopic application, this can lead to low force feedback in spite of cancelling the friction, and can fatigue surgeons' muscles due to the constant effort required to operate the device. These drawbacks can be prevented by including a pre-stressed structure. Therefore, the total amount of potential energy in the system will be altered, which may lead to two situations. In the first situation, the potential energy in the system will be constant over a finite range of motion, resulting in static equilibrium over this range of motion. Therefore, no force is required to operate the system or to hold it at any position within the balanced range, and force feedback is restored. This kind of mechanism is called a statically balanced compliant mechanism (SBCM) (Herder and van den Berg, 2000). In the second situation, the potential energy in the system has two minimums, thus making the system bi-stable (e.g. the grasper will be stable in the open and in the closed positions). This enables the grasper to provide the necessary force to hold objects (e.g. tissue or a needle) for longer periods of time. Conventionally, the SBCM used spring based bi-stable mechanisms (Herder and van den Berg, 2000), leaf springs (De Lange, 2008) or bi-stable straight guided beams with compliant (Stapel and Herder, 2004; Hoetmer et al., 2009) or a partially compliant structure (Tolou and Herder, 2009) as the static balancer. However, all aforementioned works rely on preloading in a direction perpendicular to instrument actuation, and therefore protrudes outside the grasper and is difficult to be tuned for fabrication errors and improved performance. Collinear preloading has only been introduced in a few studies for other applications, such as: human skeleton (Chen and Zhang, 2011), MEMS (Tolou et al., 2010b) and precision stages (Dunning et al., 2011).

This article presents a laparoscopic 2DoFs robotic arm with a statically balanced fully compliant laparoscopic grasper (namely SBCG) as the end effector. The design is a step toward the development of fully compliant robotic arms. The 2DoF robotic arm was designed with internal motors actuating the DoFs. The grasper was designed as a monolithic structure, where the positive stiffness was cancelled using pre-curved straight guided beams as static balancers. The concept allows the static balancers to be integrated inside the compliant grasper, to be tuned for fabrication errors, and to be adjusted for different force displacement behaviors: bi-stable, zero stiffness with near zero actuation force, constant positive force and constant negative force. The performance of the novel SBCG and the laparoscopic robot will be investigated experimentally.

The remainder of this paper is structured as follows: in Sect. 2 the concepts of the robotic arm and SBCG are presented and followed by Dimensional Design, Fabrication and Measurement in Sect. 3. Results are presented and discussed in Sect. 4. Finally, conclusions are made in Sect. 5.

2 Conceptual design

2.1 Robotic arm

The robotic arm is conceived to be used as an extension of traditional laparoscopic tools, endoscopes, and existing robotic arms. This results in two main design criteria: increasing the DoFs, thus the dexterity of the system, and making the operation in narrow space easier. An example of the intended application and a 3-D sketch of the robotic arm are shown in Fig. 1. The robotic arm is jointly attached to a traditional laparoscope to increase the dexterity. In addition, the robotic arm could magnetically or mechanically be coupled to the abdominal wall. The proposed design for the

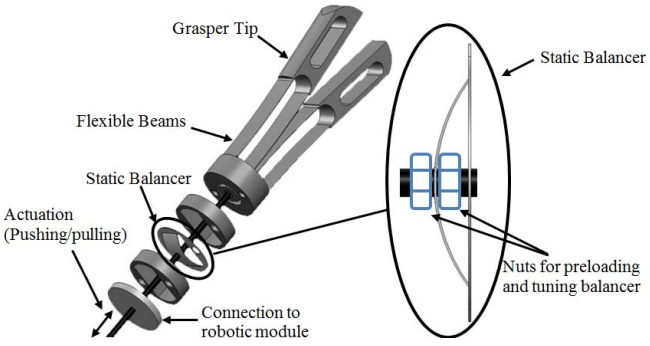

Figure 2. 3-D sketch of the SBCG at relaxed configuration.

robot arm is serial. This implies that the robotic arm can be easily integrated with traditional tools, thanks to its cylindrical shape. The robotic arm provides two additional DoFs as well as the actuation of the SBCG. The proposed design is a 2DoFs cylindrical link embedding two rotational motors and respective mechanisms, for pitch and roll DoFs.

Regarding the actuation of the compliant grasper, a cable actuation system is proposed. One end of the actuating wire is attached to the central beam of the compliant grasper, thus when the cable is pulled the grasper is closed, as explained in Sect. 3.1.2. The other end of the wire is attached to a winding rod. Cable actuation exhibits several advantages: the actuator can be placed remotely, i.e. outside the part of the instrument that is inserted into the patient, thus not influencing the dimensions of the robotic arm. An external spring is used to let the cable spring back to its natural position. The spring also ensures that the cable is always tensioned.

2.2 Statically balanced compliant grasper

The design of the compliant grasper has been inspired from the work of (Herder and van den Berg, 2000). The initial (i.e. relaxed) configuration of the compliant grasper is half open, to reduce the stresses in both the compliant grasper and the static balancer (see Fig. 2). The opening and closing of the compliant grasper corresponds to actuation by pushing or pulling the middle beam as shown in Fig. 2. In Fig. 3a, the force-displacement curve of the grasper is linear with a positive stiffness and passes through the origin; the origin of the graph refers to the relaxed configuration of the grasper. The closed position of the compliant grasper is marked A. B is the equilibrium position where the compliant grasper is half open and relaxed. C indicates the open position of the compliant grasper.

To statically balance the compliant grasper, negative stiffness should be added to compensate the positive stiffness of the device (Herder, 1998). Consequently, near zero stiffness with a near zero actuation force may be achieved. Bi-stable compliant mechanisms have been an interesting mechanism with nonlinear stiffness behavior (Jensen et al., 2001; Hartono, 2001; Qiu et al., 2004; Li and Zhou, 2005; Sönmez,

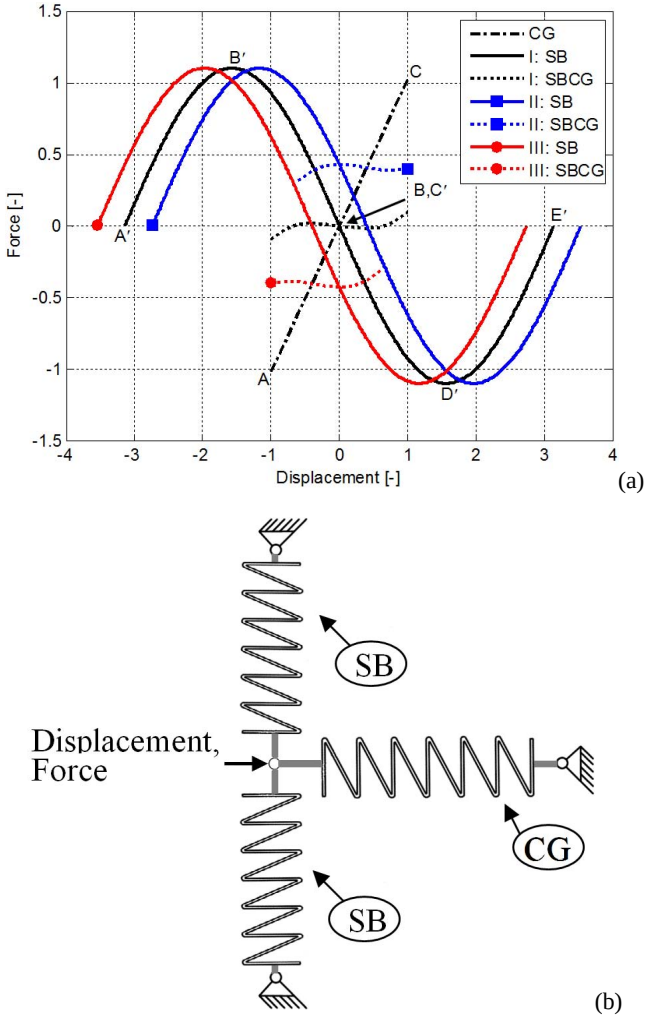

Figure 3. **(a)** The force-displacement curve and **(b)** the corresponding configuration of a typical bi-stable mechanism (static balancer, SB) and the compliant grasper (CG) as a pin-pin bi-stable linear compression spring mechanism and a linear extension spring respectively. The shown configuration in **(b)** corresponds with position B of **(a)**. **(a)** also shows the different cases (I–III) of zero stiffness with zero (black lines), constant positive (blue lines ■) and constant negative actuation force (red lines •). Force-displacement behaviors accomplished by positioning the center of the static balancer (SB) relative to the compliant grasper (CG). Positioning the unstable equilibrium (C′) can be performed by nuts.

2008; Todd et al., 2010). It has been shown that these mechanisms have the largest ratios of both compensated force and statically balanced stroke relative to the size (Dunning et al., 2011). A typical force-displacement curve of such a mechanism is shown in Fig. 3a. For clarity, in this figure the bi-stable mechanism and the grasper considered as pin-pin linear springs: a bi-stable compression spring mechanism and an extension spring respectively (Fig. 3b). In Fig. 3a, five points are identified in the force-displacement curve of the bi-stable mechanism: first stable equilibrium position (A′),

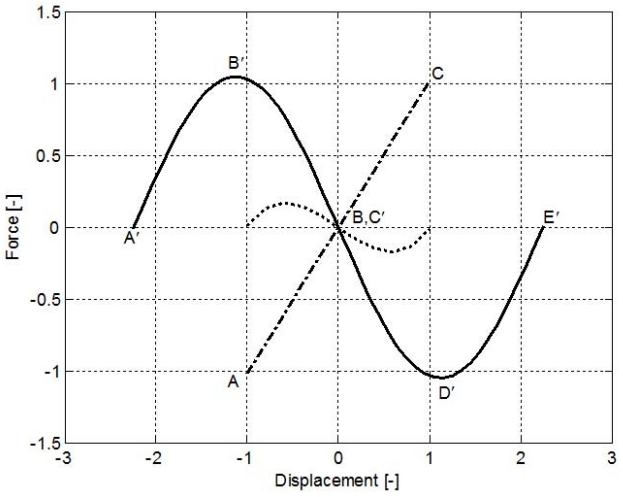

Figure 4. Conceptual dimensionless force-displacement behavior of statically balanced compliant grasper (SBCG) for the case of bi-stable behavior. Force-displacement behaviors accomplished by using stiffer balancer; stiffness of the static balancers may be adjusted by varying thicknesses and initial shape.

initial buckling (first bifurcation point) (B′), unstable equilibrium point (C′), snap through (second bifurcation point) (D′), and the second stable equilibrium point (E′). The negative stiffness of bi-stable mechanism (B′-D′) is tuned to have the same stiffness as the compliant grasper (A-C) but with the opposite sign. The cooperative action of force-displacement behaviors of the grasper and bi-stable mechanism can result into cases of zero stiffness with (I) zero actuation force, (II) constant positive force and (III) constant negative force as shown in Fig. 3a or (IV) bi-stable behavior (Fig. 4). Case I (black dotted line) occurs when the unstable equilibrium position (C′) of the bi-stable beam (black solid line) falls on the equilibrium position of the grasper (B; black dash dotted line). Case II (blue dotted line ■) occurs when the unstable equilibrium position (C′) of the bi-stable beam (blue solid line ■) falls after the equilibrium position of the grasper (B; black dash dotted line). Case III (red dotted line •) occurs when the unstable equilibrium position (C′) of the bi-stable beam (red solid line •) falls before the equilibrium position of the grasper (B; black dash dotted line). Case IV occurs when the negative stiffness of the static balancer (B′-D′) is greater than the positive stiffness of the grasper (A-C; i.e. over compensation). More on this subject can be found in Tolou et al. (2010b) and Pluimers et al. (2012).

In this research, straight guided beams with initially precurved shape were employed as the bi-stable mechanism. However, in practice the buckling behavior of such beams are not symmetric (opposite to Fig. 3a) because of the fixed-guidance at the end tips. The proposed concept presents a straightforward method to preload the structure along the axis, unlike the conventional ones that are preloaded orthogonal to the direction of instrument actuation (Hoetmer et al., 2009); therefore, the final design is more compact. The method presented here is also capable to be tuned for relevant force displacement behaviors I–IV. This can be accomplished by using the nuts shown in Fig. 2. To study the functionality of this concept for different balancers, a modular design was made and illustrated in Fig. 2.

3 Dimensional design and fabrication/measurement

3.1 Robotic module

3.1.1 Medical requirements

Medical professionals estimate that a force of 5–10 N and a minimum speed of 360 ° s^{-1} are needed during surgical tasks in traditional robotic surgery to perform all possible tasks. As a result, a typical manipulator requires a total power of up to 4 W. These requirements are less strict when specific manipulation tasks are performed (Parittotokkaporn et al., 2010).

3.1.2 Actuation system and control

The robotic arm provides two additional DoFs as well as the actuation of the compliant grasper. According to medical requirements, a suitable diameter for the robotic modules should be slightly less than 12 mm to be inserted through a 12 mm internal diameter laparoscopic trocar. Two SBL04 micro motors (Namiki, Akita, Japan) were selected as actuators for the 2 DoFs because of their small size (4 mm in diameter and 17.4 mm in length including the gearbox) and large torque (up to 5.7×10^{-3} Nm). One motor drives an off-the-shelf 3 mm diameter worm gear (Didel, Belmont, Switzerland), which is used to transmit motion between the axis of the motor and the orthogonal pitch joint axis. The other motor is used for the roll mechanisms. It drives two modulus 0.3 spur gears with unitary transmission ratio. The robotic arm has a total length of 41.8 mm excluding the grasper.

A Faulhaber motor has been used to pull a steel cable inside a 1 mm sheath. When activated the motor closes the grasper by pulling the cable. When the motor is idle, the passive opening of the compliant grasper is due to a compression spring, placed between the compliant grasper and the tip of the robotic arm, as shown in Fig. 7b. If the compliant grasper is not perfectly balanced and has a small residual positive stiffness or force, the spring may be neglected.

A control strategy based on the preemptive priority pseudokernel approach was selected to drive multiple brushless DC motors in real time using one microcontroller instead of utilizing one chip dedicated to each motor (Susilo et al., 2009). The Faulhaber motor is driven thanks to its commercial driver.

3.1.3 Manufacturing

This model was produced using rapid prototyping techniques (VisiJet XT 200 and Invision Si2, Inition, ThingLab, London, UK). An acrylic material composed of urethane acrylate polymer (35–45 %) and triethylene glycol dimethacrylate ester (45–55 %) was used. At this stage, both devices were tested separately. Integration between working prototypes remains relevant and will be done once they are manufactured in final form.

3.2 Statically balanced compliant grasper

3.2.1 Scaling

To evaluate the proposed concept (see Sect. 2.2), a prototype was made. Similar to the robotic arm, the diameter of the compliant grasper must be slightly smaller than 12 mm. For ease of prototype fabrication and verification, the model was scaled up by 3.5 times. The model maintained the stiffness and stresses of the small scale compliant grasper during scale-up. The stiffness (k), in a flexible part is dependent on the length (l), thickness (b), and height (h) of the model, as shown in the force-moment relations based on the deflection of a cantilever beam with end load (Gere and Timoshenko, 1999) (where "I" is the area moment of inertia):

$$\delta = \frac{Fl^3}{3EI} \rightarrow k = \frac{F}{\delta} = \frac{3EI}{l^3}$$
$$\text{with : } I = \frac{bh^3}{12} \rightarrow k = \frac{Ebh^3}{4l^3} = \frac{Eb}{4}\left(\frac{h}{l}\right)^3 \quad (1)$$

As can be seen in Eq. (1), the stiffness remains the same if the length and height are scaled with the same ratio. Therefore, all the geometrical values of both the compliant grasper and the static balancer were scaled up, except the thickness. The stresses were kept the same by scaling up the actuation displacement with the same ratio as the geometrical dimensions. Because the stiffness remained constant, the force increased with the same ratio as the actuation displacement. Since the force was scaled up with the same factor as the geometrical dimensions, the stresses maintained the same. With these new values, the opening displacement of the 3.5-times scale-up compliant grasper could be calculated.

3.2.2 Finite element modeling

To provide a basis for concept evaluation, finite element modeling (FEM) was performed using the commercial FEM package ANSYS™ 11.0, and the forces-displacements behaviors were analyzed (ANSYS Inc. Version 11.0 Manual). Because of large deflections, a non-linear static analysis has been performed. PLANE82 and BEAM3 elements were used to mesh the grasper and the static balancer, respectively. The first element type consist of 2-D eight node elements with two translational degrees of freedom per node. It provides more accurate results for mixed (quadrilateral-triangular) automatic meshes and can tolerate irregular shapes without significant loss of computational accuracy. The uni-axial BEAM3 elements require the least amount of computation time, while the actual out-of-plane properties can also be provided using the real constant capability of ANSYS™. The BEAM3 element has three degrees of freedom at each node with tension, compression, and bending capabilities. The material is assumed to be isotropic and to follow linear elastic stress-strain behavior.

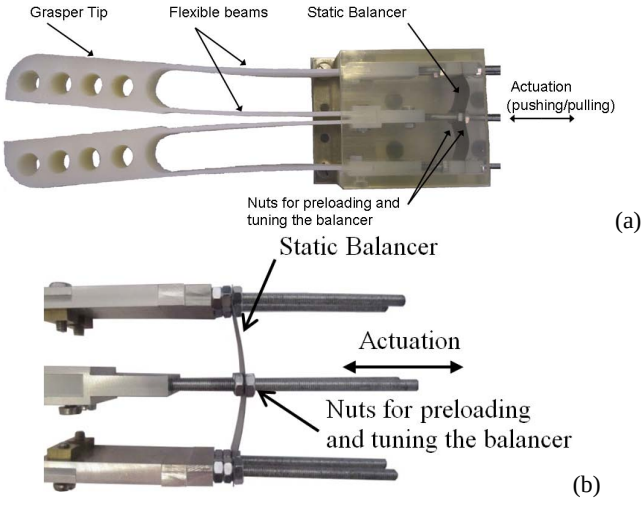

Figure 5. **(a)** Prototype of scaled up SBCG with **(b)** a detail of the tuning equilibrium positions using the nuts.

3.2.3 Manufacturing

The first prototype of the SBCG (see Fig. 5) was made using a 3-D printer (Solido SD300 Pro). The printer uses PVC sheets (0.168 mm thick, $E = 3.37\times10^9$) to build up the model. The balancers were cut out of a high quality stainless steel (ST 301) sheet, instead of using 3-D printer and PVC material, to avoid material hysteresis. The thickness was chosen to be between 0.15 ± 0.05 mm. The location of the center of the balancer was made adjustable with respect to the grasper using two nuts that are attached to a screw thread, as shown in Fig. 5. This allowed for preloading and aligning the center of unstable equilibrium for the static balancer (point C′ in Fig. 3) with stable equilibrium of the compliant grasper (point B in Fig. 3). The screw thread was also used for actuating the SBCG. The sides of the balancer were attached to the grasper via two other screw threads and nuts.

3.2.4 Measurement

Prototype verification was conducted by measuring the force-displacement curves of the compliant grasper and the SBCG. The prototype was mounted on the setup shown in Fig. 6. The compliant grasper was attached to the force

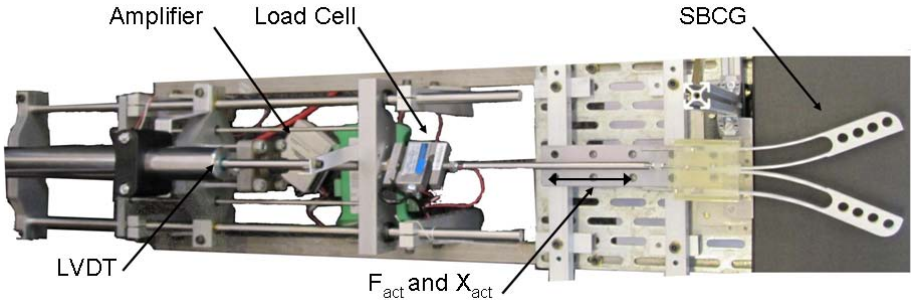

Figure 6. The top view of test set-up: the stiffness characteristic and force displacement of SBCG was determined by measuring actuation force (Fact; using a load cell) and displacement (Xact; using LVDT) during opening and closing of the SBCG.

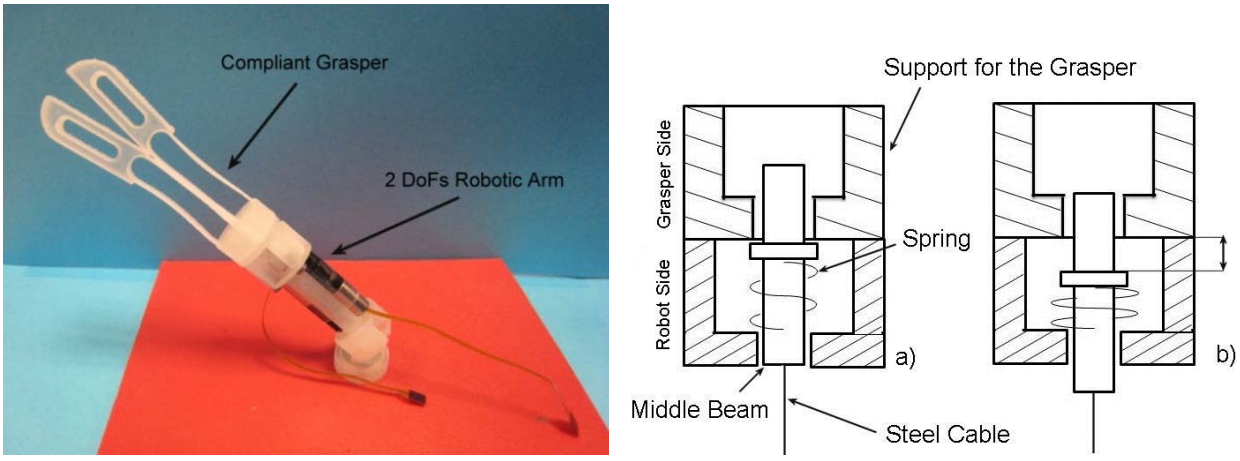

Figure 7. **(a)** Fabricated robot and grasper mock-up prototypes; **(b)** Mechanisms for coupling the grasper to the robotic arm, a) initial configuration; b) actuated configuration.

sensor by a pulling rod. For each experiment, the compliant grasper was first brought from its relaxed to its closed position. Then the compliant grasper was brought to its fully opened position and back to its closed position. During this movement, the pushing/pulling force (FETE RIS components – B3G-C3-50kg-6B, resolution = 0.06 N, range = [0,50] kg) and displacement (Positek – P101.200CL100, resolution: 0.045 mm, range = [0,200] mm, namely LVDT) were measured. An amplifier (Scaime CPJ 25) and DaQ-mx Data Acquisition system (NI USB6008) were used to read the data.

3.3 System integration

The SBCG has been mechanically integrated on the robotic arm. For this purpose, the proximal end of the grasper has been designed to fit the roll mechanisms of the robotic module. The result of the integration of the mock-up prototypes is shown in Fig. 7. The mechanism for coupling the SBCG to the robot is detailed in Fig. 7b. A double silicone coating should be added once the robot is in its final version to meet the sterilization requirements.

Although the single devices have been demonstrated separately, the whole system will be tested in the future to assess the overall performance in terms of dexterity and capability of generating proper forces for each DoF (pitch, roll, grasping) in a real working scenario.

4 Results and discussion

The limited size of the robot strictly affects the torque and speed with respect to bigger devices. The evaluation of these parameters is very important for the characterization of the whole system. Torque, speed and precision results have been adapted to the current robot design on the basis of the work described in Tortora et al. (2011) and are summarized below. The measured pitch torque is up to 14.6 mNm with a reduction 1:79, whereas the rotation torque is up to 4.35 mNm. Maximum speeds of $90\,^{\circ}\,s^{-1}$ for the pitch and of $190\,^{\circ}\,s^{-1}$ for the roll were obtained. The pitch ranges from 0° to 180°, depends only on the supported torque on the pulling cable and can be considered unlimited. The values are affected by the manufacturing of the first prototype of the robot, which has been obtained using rapid prototyping. Specifically, the

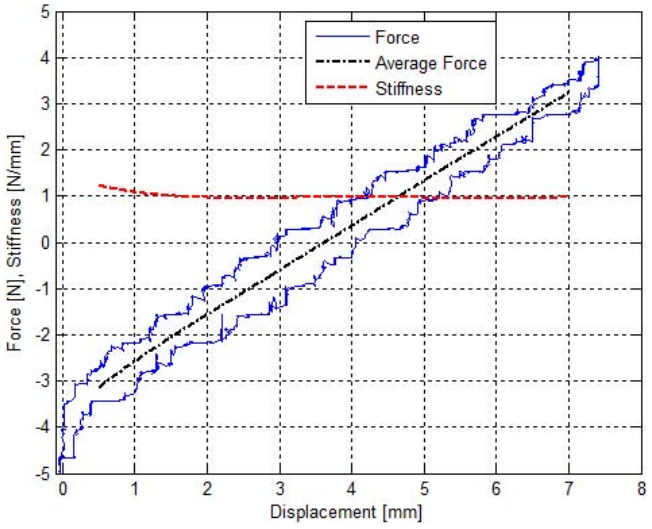

Figure 8. Force-displacement and stiffness curves of the compliant grasper from the measurement.

acrylic material has low-performance mechanical properties at the moment. Further experiments with the current design will be carried out once the robot is manufactured in a more suitable material (e.g. aluminium or titanium) and the SBCG is integrated. In this case, higher torques and speed are expected.

In Figs. 8 and 9, the force-displacement (solid line), the average force-displacement (dashed-dotted line), and stiffness-displacement (dashed line) curves of the compliant grasper and SBCG are shown, respectively. For each measurement the force-displacement of both pushing and pulling were recorded because of hysteresis, and the average was made for ease of design. The average force has been calculated by fitting a polynomial to the curves at the intervals of [0.5 7] mm, [0.3 4.7] mm and [0.2 5.45] mm and of the orders 5 N, 5 N and 7 N for Figs. 8 and 9a and b, respectively. The stiffness has been calculated by differentiating the average force. As shown in the force-displacement curve of the compliant grasper depicted in Fig. 8, the grasper has a positive constant stiffness of 1 N mm^{-1}. In Fig. 9, the results of the combined compliant grasper and static balancer can be seen. Figure 9a shows the compliant grasper with the 0.1 mm static balancer. The result is a zero stiffness, near zero with constant positive force SBCG for a range of about 5 mm. This means the negative stiffness of the static balancer is equal to the positive stiffness of the compliant grasper, but the unstable equilibrium position of the static balancing mechanism falls slightly after the equilibrium position of the compliant grasper (Case II). When the displacement becomes larger than 5 mm, the force suddenly increases as the static balancer has reached the end of its working range in which it can balance the grasper (between B′ and D′ of Fig. 3). After this point, the balancer no longer has a negative stiffness, so

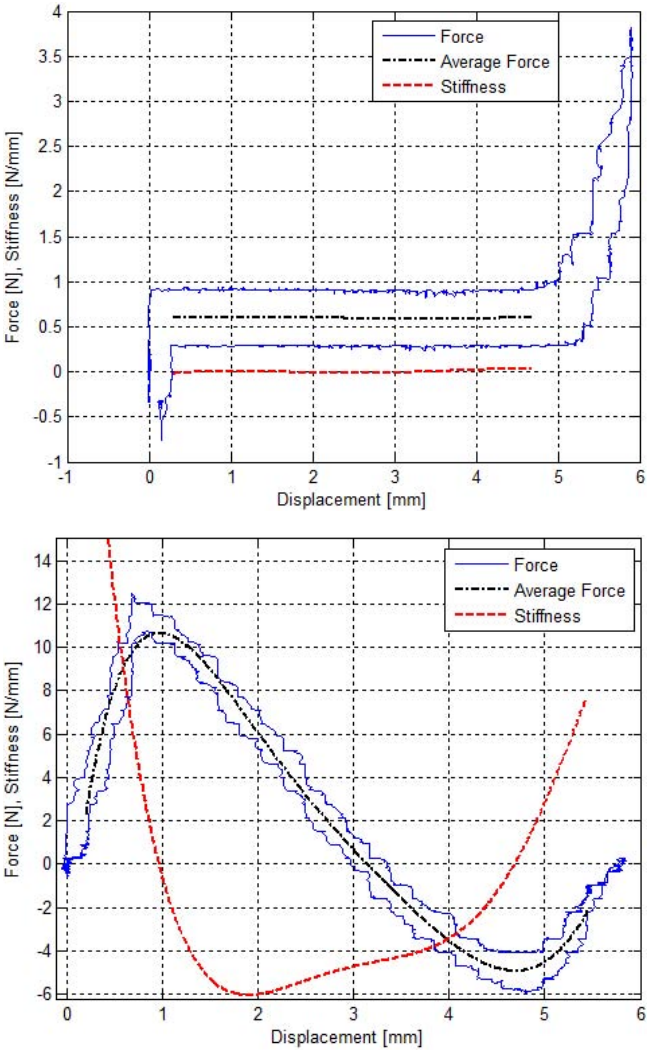

Figure 9. Force-displacement and stiffness curves of the SBCG for **(a)** statically balanced and **(b)** bi-stable behaviors from the measurements; **(a)** the compliant grasper was balanced with the 0.1 mm thickness static balancer and **(b)** the compliant grasper was balanced with the 0.15 mm thicknes static balancers.

the total force increases instead of remaining constant. Again the graph shows hysteresis of about 0.6 N. Due to the limited adaptability of the prototype, the compliant grasper could not be perfectly balanced. However, zero stiffness and near zero actuation force has been achieved.

Figure 9b shows the compliant grasper combined with the 0.15 mm static balancer. This graph shows a bi-stable behavior of the SBCG in a range of 5.8 mm due to over compensation. In all the figures hysteresis of about 1.5 N can be seen. The hysteresis could occur due to slight damping in the measurement setup (friction introduced by bearings, sliding joints and positioning sensor) and the material. The difference in the hysteresis might be explained by the magnitude of the force in the direction of actuation. It can be seen that the larger the force in this direction, the larger the hysteresis.

It should be noted that for the larger scale, both the static balancer and the compliant grasper worked successfully. However, in this scale, the static balancer has a thickness of 0.1 mm, thus the smaller model requires a static balancer of the thickness of approximately 0.03 mm; it remains to be seen if this is feasible. On the other hand, further investigation is needed on the minimum dimensional limitations of the grasper to support the applied forces during the surgery (i.e. robustness). For the future work, beside aforementioned issues, more research needs to be done to find suitable materials and production methods for compliant mechanisms of this scale.

5 Conclusions

In this article, a new 2DoF robotic arm with a fully compliant statically balanced grasper as the end-effector has been presented. The robotic arm provides pitch and roll degrees of freedom. The grasper as the end-effector has been designed fully compliant and is statically balanced using straight-guided beams that are preloaded collinear to the direction of grasper actuation. The prototype shows the adaptively of the grasper to the arm. The measured actuation forces of the grasper has been successfully compensated up to 94 %, and a near zero stiffness has been obtained with up to 97 % reduction. This allows the robotic arm to get force feedback from the end effector. Furthermore, bi-stable behavior is also achieved due to adjustability of the concept to some different stiffness behaviors: zero stiffness with zero (case I), constant positive (case II) and constant negative (case III) actuation forces, and the bi-stable (case IV) behavior. This design may be extended to a fully compliant statically balanced 2DoF robotic arm integrated with the current grasper.

Acknowledgements. This research is part of VIDI Innovational Research Incentives Scheme grant for the project "Statically balanced compliant mechanisms", NWO-STW 7583 and in part supported by the European Commission in the framework of the ARAKNES FP7 European Project EU/IST-2007-224565. Further thanks to R. Luttjeboer, his help was crucial in the manufacturing of the scaled up prototype.

Edited by: C. Kim
Reviewed by: two anonymous referees

References

Alterovitz, R.: Surgical Robotics, Robotics & Automation Magazine, 16, 16–17, 2009.

Breedveld, P., Stassen, H. G., Meijer, D. W., and Stassen, L. P. S.: Theoretical background and conceptual solution for depth perception and eye-hand coordination problems in laparoscopic surgery, Min. lnvas. Ther. and Allied Technol., 8, 227–234, 1999.

Chen, G. and Zhang, S.: Fully-compliant statically-balanced mechanisms without prestressing assembly: concepts and case studies, Mech. Sci., 2, 169–174, doi:10.5194/ms-2-169-2011, 2011.

De Lange, D. J. B. A., Langelaar, M., and Herder, J. L.: Towards the design of a statically balanced compliant laparoscopic grasper using topology, Proceedings ASME DETC 26th Biennial, Mechanisms and Robotics Conference, 10–13 September, Baltimore, Maryland, paper number DETC2008/MECH-49794, 2008.

Dunning, A. G., Tolou, N., and Herder, J. L.: Review Article: Inventory of platforms towards the design of a statically balanced six degrees of freedom compliant precision stage, Mech. Sci., 2, 157–168, doi:10.5194/ms-2-157-2011, 2011.

Forgione, A.: In vivo microrobots for natural orifice transluminal surgery, Current status and future perspectives, Surg. Oncol., 18, 121–129, 2009.

Fowler, D., Hu, T., Nadkarni, T., Allen, P., and Hogle, N.: Initial trial of a stereoscopic, insertable, remotely controlled camera for minimal access surgery, Surgical Endoscopy, 24, 9–15, 2010.

Gere, J. M. and Timoshenko, S. P.: Mechanics of Materials, Fourth SI edition, Stanley Thomas Publishers, Cheltenham, 1999.

Hartono, W.: On the Post-buckling Behavior of Elastic Fixed-End Column with Central Brace, ZAMM_Z. Angew. Math. Mech., 81, 605–611, 2001.

Herder, J. L.: Design of spring force compensation systems, Mech. Mach. Theory, 33, 151–161, 1998.

Herder, J. L. and van den Berg, F. P. A.: Statically balanced compliant mechanisms (SBCM's), an example and prospects, Proceedings ASME DETC 26th Biennial, Mechanisms and Robotics Conference, 10–13 September, Baltimore, Maryland, paper number DETC2000/MECH-14144, 2000.

Hoetmer, K., Kim, C., and Herder, J. L.: An extended building block approach for the design of statically balanced compliant mechanisms, 2009 ASME International Design Engineering Technical Conferences, 30 August–2 September 2009, San Diego, California, Paper number DETC2009-87451, 2009.

Howell, L. L.: Compliant Mechanisms, New York, Wiley, 2001.

Hu, T., Allen, P. K., Hogle, N. J., and Fowler, D. L.: Insertable Surgical Imaging Device with Pan, Tilt, Zoom, and Lighting, Int. J. Robot. Res., 28, 1373–1386, 2009.

Jensen, B. D., Parkinson, M. B., Kurabayashi, K., Howell, L. L., and Baker, M. S.: Design Optimization Of A Fully-Compliant Bi-stable Micro-Mechanism, Proceedings of 2001 ASME International Mechanical Engineering Congress and Exposition, 11–16 November, New York, NY, 2001.

Joice, P., Hanna, G. B., and Cuschieri, A.: Errors enacted during endoscopic surgery; a human reliability analysis, Appl. Ergon., 29, 409–414, 1998.

Lehman, A. C., Berg, K. A., Dumpert, J., Wood, A. W., Visty, Q., Rentschler, M. E., Platt, S. R., Farritor, S. M., and Oleynikov, D.: Surgery with cooperative robots, Comput. Aided Surg., 13, 95–105, 2008.

Li, S. R. and Zhou, Y. H.: Post-buckling of a hinged-fixed beam under uniformly distributed follower forces, Mech. Res. Commun., 32, 359–367, 2005.

Lum, M., Friedman, D., Rosen, J., Sankaranarayanan, G., King, H., Fodero, K., Leuschke, R., Sinanan, M., and Hannaford, B.: The RAVEN – design and validation of a telesurgery system, Int. J. Robot. Res., 28, 1183–1197, 2009.

Oleynikov, D., Rentschler, M., Hadzialic, A., Dumpert, J., Platt, S. R., and Farritor, S.: Miniature robots can assist in Laparoscopic cholecystectomy, Surg. Endosc., 19, 473–476, 2005.

Parittotokkaporn, T., Degenaar, P., Davies, B. L., and Baena, R.: Force vs. Displacement during Tool Insertion: Techniques and Modeling Approaches, Proc. Hamlyn Symposium, 2010.

Pluimers, P. J., Tolou, N., Jensen, B. D., Howell, L. L., and Herder, J. L.: A Compliant On/Off Connection Mechanism for Preloading Statically Balanced Compliant Mechanisms, DETC2012-71509, ASME IDETC 2012, Chicago, USA, 2012.

Qiu, J., Lang, J. H., and Slocum, A. H.: Microelectromechanical Systems, A curved-beam bi-stable mechanism, 13, 137–146, 2004.

Rentschler, M. E., Dumpert, J., Platt, S. R., Lagnernma, K., Oleynikov, D., and Farritor, S. M.: Modeling, Analysis, and Experimental Study of In Vivo Wheeled Robotic Mobility, IEEE T. Robot., 22, 308–321, 2006.

Stapel, A. and Herder, J. L.: Feasibility study of a fully compliant statically balanced laparoscopic grasper, Proceedings ASME Design Engineering Technical Conferences, 28 September–2 October, Salt Lake City, Utah, DETC2004-57242, 2004.

Sönmez, T. C. C.: A Compliant Bistable Mechanism Design Incorporating Elastical Buckling Beam Theory and Pseudo-Rigid-Body Model, J. Mech. Design, 130, 042304-1/13, 2008.

Susilo, E., Valdastri, P., Menciassi, A., and Dario, P.: A miniaturized wireless control platform for robotic capsular endoscopy using advanced pseudokernel approach, Sensor. Actuat. A-Phys., 156, 49–58, 2009.

Todd, B., Jensen, B. D., Schultz, S. M., and Hawkins, A. R.: Design and Testing of a Thin-Flexure Bistable Mechanism Suitable for Stamping From Metal Sheets, J. Mech. Design, 132, 071011-1/7, 2010.

Tolou, N. and Herder, J. L.: Concept and Modeling Of A Statically Balanced Compliant Laparoscopic Grasper, in: Proceeding of ASME 2009 International Design Engineering Technical Conferences and Computers and Information in Engineering Conference, 30 August–2 September, San Diego, CA, USA, Paper no. DETC2009-86694, 163–170, doi:10.1115/DETC2009-86694, 2009.

Tolou, N., Gallego, J. A., and Herder, J. L.: Statically Balanced Compliant Micro Mechanisms (SBMEMS): A Breakthrough in Precision Engineering, Mikroniek, 50, 20–25, 2010a.

Tolou, N., Henneken, V. A., and Herder, J. L.: Statically Balanced Compliant Micro Mechanisms (SB-Mems): Concepts And Simulation, in: Proceeding of ASME 2010 International Design Engineering Technical Conferences and Computers and Information in Engineering Conference, 15–18 August 2010, Montreal, Quebec, Canada, Paper no. DETC2010-28406, 447–454, doi:10.1115/DETC2010-28406, 2010b.

Tortora, G., Dimitracopoulos, A., Valdastri, P., Menciassi, A., and Dario. P.: Design of Miniature Modular in vivo Robots for Dedicated Tasks in Minimally Invasive Surgery, AIM 2011, Budapest, Hungary, 3–7 July 2011.